

SqueezeSAM: User-Friendly Mobile Interactive Segmentation

Balakrishnan Varadarajan Bilge Soran Forrest Iandola Xiaoyu Xiang
Chenchen Zhu Yunyang Xiong Lemeng Wu Raghuraman Krishnamoorthi
Vikas Chandra

{balakv,bsoran,fni, xiangxiaoyu,yunyang,chenchenz,lmwu,raghuraman,vchandra}@meta.com

Abstract

The Segment Anything Model (SAM) has been a cornerstone in the field of interactive segmentation, propelling significant progress in generative AI, computational photography, and medical imaging. Despite its ability to process arbitrary user input and generate corresponding segmentation masks, SAM’s 600 million parameter architecture, based on ViT-H, is not compatible with current mobile hardware due to its high computational demands and large model size. Our research aims to adapt SAM for use in mobile photography applications. To this end, we have developed a fully convolutional SqueezeSAM model architecture, which is 62.5 times faster and 31.6 times smaller than the original SAM, making it a viable solution for mobile applications. Furthermore, our tiny model achieves an mIOU within 1% of the original ViT-H architecture.

Automated segmentation holds significant value in the creation flow for photography applications, as evidenced by its adoption by leading industry players like apple and capcut. To facilitate this automation, we employ salient object detection and simulate potential user clicks for foreground object selection, generating an initial segmentation mask that users can subsequently edit interactively. A common user expectation is that a click on a specific part of an object will result in the segmentation of the entire object. For example, a click on a person’s t-shirt in a photo should ideally segment the entire person, not just the t-shirt. However, SAM typically only segments the clicked area. We address this limitation through a novel data augmentation scheme. Consequently, if a user clicks on a person holding a basketball, both the person and the basketball are segmented together, aligning with user expectations and enhancing the overall user experience.

1. Introduction

Since the introduction of the Segment Anything Model (SAM) [15], it has catalyzed significant advancements in generative AI, medical imaging, and computational photog-

raphy [27, 33, 45]. Our research focuses on interactive segmentation, a feature that enables users to select and extract objects within images on a smartphone. This functionality has already been implemented in the iPhone with iOS 16, but the proprietary model used by Apple is not available for retraining by researchers. Our objective is to develop an open-source, fast, user-friendly, mobile model for interactive image segmentation.

The adoption of automated segmentation by major industry players underscores its substantial importance for photography applications like apple and capcut. SAM requires the user to initiate the segmentation process by clicking on an object. To overcome this, we propose using salient object detection (SOD) to select a few interesting points in the image, enabling SAM to generate an initial segmentation that can be refined through user input. As SOD aims to identify objects and regions that attract human attention, it is logical to use it to predict the image regions that humans are likely to click on.

Another challenge with SAM is its latency -it takes half a second on an A100 GPU and over ten seconds on an iPhone CPU. Local device operation is crucial for interactive latency and privacy preservation. The latency of SAM is primarily due to its encoder, a ViT-H vision transformer [8]. While more efficient SAM variants exist, they significantly compromise the quality-of-results [1, 3, 47, 48]. In our work, we explore model architectures and training schemes that offer low latency while maintaining a quality-of-results competitive with the original SAM model. We also show that our models deliver higher quality segmentation of salient objects.

In summary, our novel contributions include a new model architecture that is 62.5 times faster and 31.6 times smaller than the original SAM, and the ability to generate segmentation masks for salient objects without user inputs. We will also publicly release the weights of our compact model, trained on 1 billion masks and 11 million images.

2. Related work

Interactive segmentation is a task where a user clicks

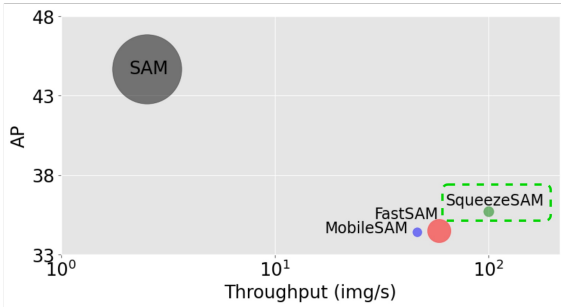
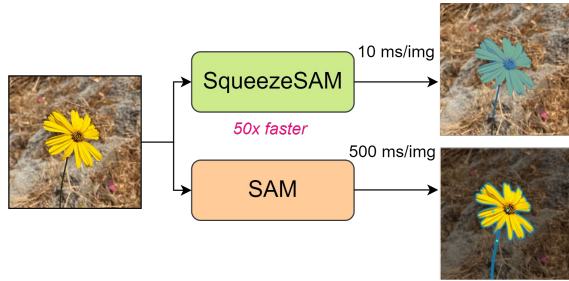


Figure 1. A comparative analysis of SqueezeSAM and SAM. (Top) Speed comparison between SqueezeSAM and SAM on a single NVIDIA A100 GPU. (Bottom) Performance/Runtime/Parameter comparison of SAM and other efficient models.

on interesting regions of an image, and a computer vision model segments those regions. From the 1980s through the early 2010s, Snakes [14], GraphCut [2], and Geodesic Star [10] applied classical computer vision techniques to this problem. Then, deep learning spread from object classification [17] to semantic segmentation [26] to interactive segmentation [42].

By 2022, the de facto approach to interactive segmentation was the following. The model architecture consisted of a Vision Transformer (ViT) [8, 36] or ConvNet encoder plus a feature pyramid network decoder [22]. The training set incorporated COCO [21], LVIS [11], and possibly a few other instance segmentation datasets. Evaluation datasets included LVIS and DAVIS [46]. To evaluate the model, a standardized algorithm simulates mouse-clicks on an image, and it stops clicking when the generated segmentation masks achieve an intersection over union (IOU) of 0.9. The fewer clicks to achieve 0.9 IOU, the better. In this regime, the leading models included FocalClick [4], SimpleClick [23], and RITM [35]. To segment images with 0.9 IOU, SOTA deep neural networks require 5 times fewer clicks than classical approaches [35].

Segment Anything Model (SAM) has significantly advanced the field of interactive segmentation [15]. Like SimpleClick, SAM employs a ViT encoder. However, in contrast to SimpleClick’s feature pyramid network decoder,

SAM utilizes a Transformer-based decoder. The most notable departure of SAM from previous work is its training on a novel dataset, SA-1B, comprising 11 million images and 1 billion masks. This new dataset was instrumental in enabling SAM to surpass FocalClick, SimpleClick, and RITM in both interactive and instance segmentation benchmarks.

Much work has been built on top of SAM. SAM is core to generative AI tasks including style transfer [24, 29], image inpainting [45], text guided image and video editing [39, 41], and 3D reconstruction and generation [33, 34]. Further, SAM has been applied to general medical image segmentation [27] and specialized tasks like polyp segmentation [49], skin lesion segmentation [40], and COVID-19 lung imagery [5]. Improvements to the quality and efficiency of SAM will benefit all of these applications.

Alternative SAM model architectures have been proposed for faster inference. While SAM uses a large vision transformer called ViT-H, MobileSAM uses the ViT-tiny encoder model [47]. Others use convolutional encoder models: FastSAM uses a variant of the YOLOv8 encoder architecture [13, 48], and NanoSAM uses ResNet18 [1, 12]. EfficientViT uses an encoder that includes transformers and convolutions [3]. To avoid the high cost of training from scratch on the SA-1B dataset, MobileSAM, NanoSAM, and EfficientViT train via distillation from SAM. FastSAM trains on a small subset of the SA-1B dataset.

Salient Object Detection (SOD) involves predicting a heat map that distinguishes between salient and non-salient image regions. ¹ Since 2010, several SOD benchmark datasets have emerged. In most benchmark datasets, humans label the ground-truth masks using a graphical interface [28, 37, 43]. Some datasets also incorporate human eye tracking data into the labeling process, based on the premise that areas of fixation are likely to be salient [18, 44]. Top performing models on SOD benchmarks include R³Net [7], U²Net [30], and SSOM [6]. Notably, SSOM employs SAM to enhance salient object detection. In a related vein, our research utilizes SOD to augment interactive segmentation.

3. Proposed approach

The task of zero-shot instance segmentation using user clicks can be formally defined as follows. Given an image $\mathbf{I} \in \mathbb{R}^{3 \times H \times W}$ and a set of user clicks $\mathbf{u} = (x_c, y_c)_{c=1, |C|}$, the segmentation problem is to provide the probability of every pixel in the image belonging to the mask as $p(b_{ij} | (x_c, y_c)_{c=1, |C|})$.

The original SAM model consists of an encoder \mathcal{E} and a decoder \mathcal{D} . Given an image \mathbf{I} , the encoder first embeds the image into an rich intermediate representation $\mathbf{x} = \mathcal{E}(\mathbf{I})$.

¹To dispel a common point of confusion: While object detection typically means bounding boxes, SOD uses masks.

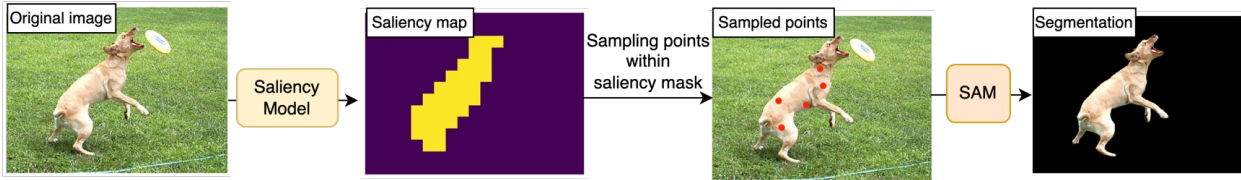


Figure 2. **Salient SqueezeSAM pipeline.** Salient Object Detection feeds initial points to SqueezeSAM, so the user can get an initial segmentation without clicking on the screen. After that, the user can interactively edit and improve the segmentation. It runs in real-time on an iPhone.

The decoder (typically light weight) consumes the intermediate representation \mathbf{x} and an external user input \mathbf{u} to produce a set of k segmentation mask $\mathbf{m} \in \mathbb{R}^{H \times W \times k}$ along with their estimated IOU scores $s \in \mathbb{R}^k$. The proposed idea of early fusion combines the input to the encoder with user clicks as $\mathbf{I} \times \mathbf{u}$. We will summarize the motivations for early fusion in the next few sections.

3.1. SqueezeSAM Encoder-Decoder Architecture

Our initial exploration began with using a ViT tiny backbone (as an alternative to ViT-H) trained on the SA-1B dataset. Due to the difficulty in quantization and deployment of ViT tiny models, subsequently, we also explored a UNet based architecture and discovered that we can train efficient and high quality models easily using a UNet backbone without much architecture tuning. We show our end-to-end model architecture in Figure 3. The inputs to our model are an image $\mathcal{I} \in \mathbb{R}^{3 \times 1024 \times 1024}$ and a set of clicks.² The model’s computational footprint is dominated by the SqueezeSAM encoder and decoder. In Figure 4, we show the precise layers and dimensions of our encoder and decoder, and we show the details of the DoubleConv blocks in Figures 5 and 6. Here are a few key design choices we made and why we made them:

- **Apply transformers at the bottom scale of the UNet.** We downsample the image from $1024 \times 1024 \times 3$ all the way down to $1 \times 1 \times 256$. We then apply two transformer layers on the $1 \times 1 \times 256$ representation. This is informed by papers such as SnapFusion [20] and NASViT [9], which find that when combining convolutions and transformers, the best speed-accuracy tradeoff is achieved by using transformers in the lower-resolution layers.
- **Low channel count.** In addition to optimizing for latency, we wish to maintain a small model size to avoid wasting storage space on the smartphone. So, while some UNet models double the number of channels each time they downsample (going over 1000 channels) [20], we

²For now, let’s assume the clicks are from a user clicking a mouse or tapping a smartphone screen. In Section 5, we will explain how to use salient object detection to synthesize clicks.

use a maximum of 256 output channels per layer.

- **BatchNorm.** While works such as ConvNext [25] show the accuracy advantage of LayerNorm over BatchNorm, there are two computational-efficiency advantages of using BatchNorm. First, LayerNorm has a square-root operation, which we find is particularly expensive on mobile hardware (adding up to 50% to the total latency). Second, after training is complete, BatchNorm can be folded into a Conv+Bias layer, so there is no computational cost to BatchNorm inference [16]. This folding is not possible with LayerNorm.
- **Skip connections.** Following prior literature on UNet models [31], we add skip connections from the hidden layers of the encoder to the hidden layers of the decoder.

After the encoder and decoder, we adopt the Mask MLP block from original SAM. It has one small MLP for each of the 4 output channels.

3.2. Early fusion

We add the user input points as separate channels (along with the original RGB image input). In particular, these clicks are encoded as circles in the fourth channel and the bounding box is encoded as a rectangle in the fifth channel. By knowing the clicks upfront, the model is able to focus more of its attention and its parameters on the image regions that user wants to segment. In addition to this early fusion, points are also encoded using the decoder transformer (as is done with SAM). The mix of early and late fusion helps the net further in being able to attend to the sought objects.

3.3. Training

We train our models on the SA-1B dataset for 10 epochs using V100 GPUs. We use a batch size of 4 per GPU (effective batch size of 256) and synchronized batch norm applied between each of the UNET layers. During training, we sample 8 masks per image uniformly at random. An initial learning rate of $5e-4$ is followed by a linear decay is employed. The total training time takes around 7 days.

To achieve this relatively short training time on a large dataset, we changed how we feed clicks into the model dur-

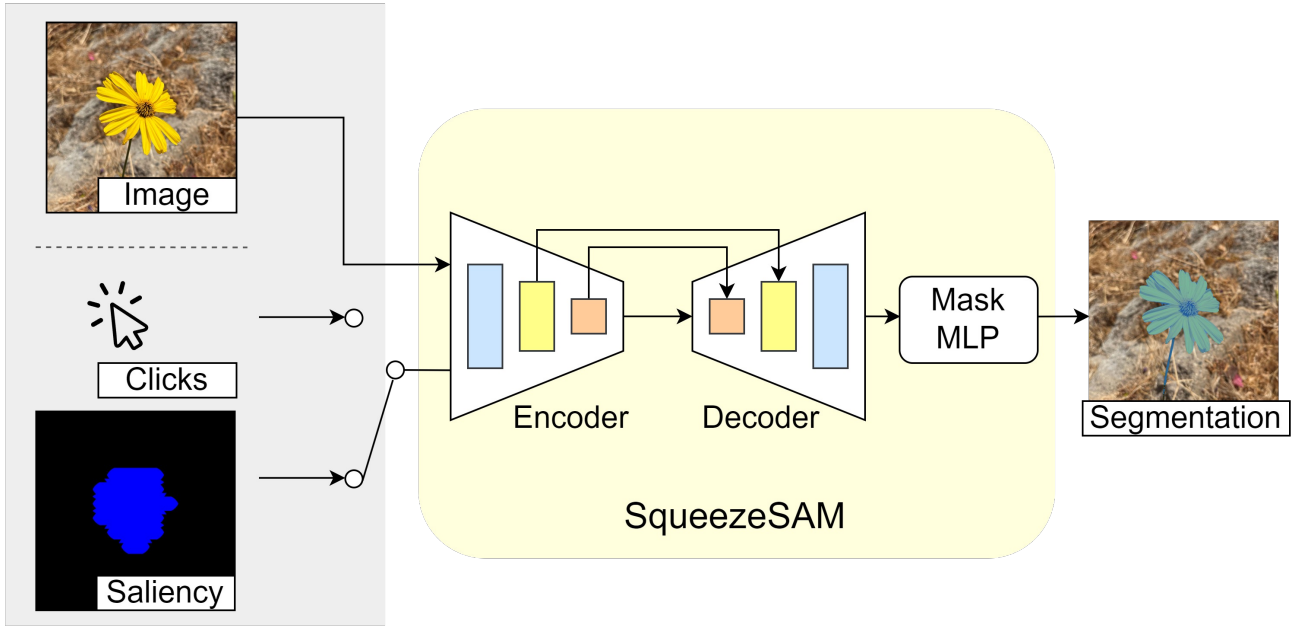


Figure 3. SqueezeSAM model architecture. Our proposed SqueezeSAM can take point coordinates from user’s clicks, or “guess” user’s intention from a saliency mask, and generate the corresponding segmentation output. For example, the model can begin by segmenting one object, and the user can interactively edit the segmentation or segment more objects.

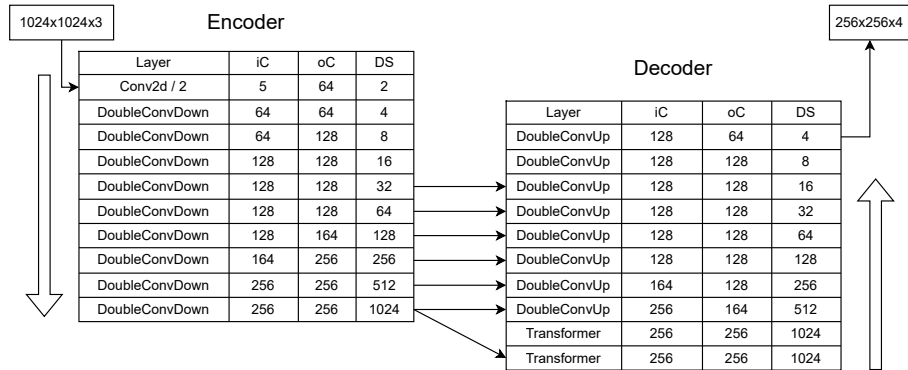


Figure 4. SqueezeSAM encoder-decoder model architecture. DoubleConv modules are described in later figures. iC = input channels from the previous layer, not including concatenated skip-connections. oC = output channels. DS = downsampling factor, relative to the original input image.

ing training. In the original SAM training, for each batch, the model runs on one click, then another click point is sampled and the model runs again. So, original SAM runs multiple steps of training for each batch of data. This inflates the training time, so for SqueezeSAM we simply input a collection of points for each batch and run one training step for each batch. Otherwise, we adhere to the original training protocol from the SAM paper.

4. Evaluation

To evaluate SqueezeSAM’s interactive segmentation capability, we choose two instance segmentation benchmarks: COCO and LVIS. Following the evaluation method of SAM [15], we take bounding boxes generated from ViT-Det [19] object detection, and we feed these bounding box into SqueezeSAM. We use the same protocol when evaluating models from the literature.

To evaluate inference latency, we select the A100 GPU and the iPhone 14 CPU. Why not evaluate on iPhone GPU

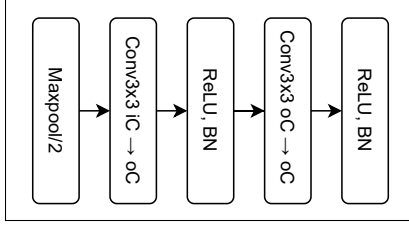


Figure 5. **DoubleConvDown** module used in the SqueezeUNet encoder.

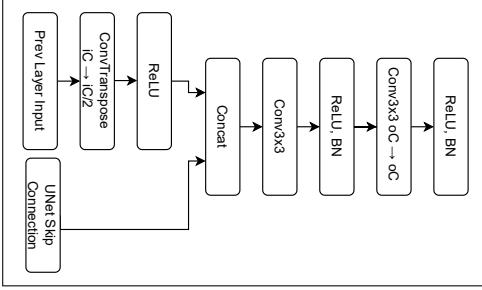


Figure 6. **DoubleConvUp** module used in the SqueezeSAM decoder. The ConvTranspose does 2x upsampling and reduces the channels by 2x.

or NPU? There are thousands of models of smartphones, hundreds of smartphone brands, and dozens of manufacturers of smartphone chips. As described in [38], mobile GPUs and accelerators are not standardized, so when deploying a model to all types of smartphones it’s easier to use the CPU.

The disk size of our model is reduced to 14MB with int8 quantization. We find that with our architecture, we find less than 1 percent drop in model quality.

In Table 1, we compare original SAM, SqueezeSAM, and MobileSAM. We observe that, relative to the other efficient models, SqueezeSAM produces higher-quality results. Our model has a UNET architecture that is trained from scratch on the SA-1B dataset. Unlike most other techniques that use tricks like pre-training and distillation, our models can get competitive performance without any of these techniques. We also find that our model has smaller latency compared to the MobileSAM version.

5. Application

The automatic generation of segmentation plays a crucial role in the development process for photography applications, as evidenced by its adoption by leading industry players such as Apple, CapCut. In line with these objectives, we explored ‘classic’ (non-interactive) instance segmentation and salient object detection (SOD) to facilitate auto-creation. Our qualitative observations indicated that SOD helped us create superior input points, leading to an en-

hanced interactive segmentation experience. An additional advantage of SOD is its ability to identify objects beyond the vocabulary of the training set, often including multiple contextually correlated objects, such as a person holding a parrot, rather than just a person or a common object. Consequently, we opted to utilize SOD in our approach.

The output of a SOD is a heatmap where the highest values of the heatmap refer to the most salient regions. To sample points from the saliency heatmap, after applying a global dynamic thresholding method like Otsu’s method [32], we detected the blobs. Most salient blob is identified with respect to the highest value within each blob, and we used the frequency of max heatmap value as a tie breaker when two blobs have the same value. After selecting the most salient blob, we divide it into 4 sections with respect the blob’s center of mass. Then we use the center of mass from each section as our selected points besides the center of mass of the whole blob, creating 5 clicks. When the center of mass lies out of the heatmap, we use the closest point within the mask. This way of sampling guarantees that the point distribution is in accordance to the blob shape. Figure 8 shows a comparison to the grid sampling.

For our application, we found that users are most interested in interactively segmenting people (and the things that people touch and hold) and pets (and dogs carrying frisbees and things like that). We call this “whole object segmentation.” However, with original SAM (or SqueezeSAM from the previous section), when you click on an object, it often segments just part of the object - see Figure 9. We address this with a series of data augmentations. And we will show that these augmentations improve performance on whole object segmentation, with the tradeoff that they reduce performance when evaluated on the original COCO and LVIS evaluation sets.

5.1. Data Augmentation

We identified some issues with the SA1B dataset that are especially detrimental to the task of whole-object segmentation on people and pets.

- **Ambiguity:** A single click may correspond to multiple objects. Although SAM has a way to mitigate this by outputting multiple masks per inference call, this is typically not enough.
- **No good representation of salient object masks.** Each image in the SA-1B dataset has a collection of masks which are mostly non central to the theme of the image.
- **Incomplete masks:** Many times the important mask in the image (example person) would be missing.

To address these issues, we use the following data augmentation techniques.

- **Mask merging.** We suppressed all masks that lie within a larger mask. For example, the models trained on the original dataset would segment out t-shirt when clicked

Table 1. Instance segmentation results, latency and number of parameters. All compared models are prompted with ViTDet boxes to do zero-shot segmentation. AP numbers are reported as all, S, M, L. AP^P denotes AP for the person category. AP and mIOU evaluation of FastSAM and EdgeSAM are from [15, 48], while the evaluation of SAM ViT-H, MobileSAM and EfficientSAM was done by the authors of this paper.

	COCO						LVIS					latency (ms)		Params(M)
	mIOU	AP	AP ^L	AP ^M	AP ^S	AP ^P	mIOU	AP	AP ^L	AP ^M	AP ^S	A100	iPhone	
SAM ViT-H [15]	78.4	46.5	61.7	51	30.8	53.5	78.9	44.7	65.5	57.6	32.5	500	-	600
MobileSAM [47]	74.3	38.7	54.3	42.2	23.7	39.0	72.3	34.4	53.7	44.9	23.8	12	-	9.7
FastSAM [48]	-	37.9	50.0	43.4	23.9	-	-	34.5	50.0	43.4	23.9	-	-	68
EdgeSAM [50]	76.7	43.0	55.1	48.9	30.3	-	76.0	-	-	-	-	-	-	9.6
EfficientSAM-Tiny [51]	75.7	42.3	57.4	46.2	26.7	-	74.3	39.9	59.9	51	28.9	19	-	10
EfficientSAM-Small [51]	77.0	44.4	60.1	48.3	28.4	-	75.4	42.3	62.3	54	30.8	21	-	25
SqueezeSAM (fp32)	77.9	41.1	57.0	45.1	25.1	44.5	78.1	37.4	58.0	49.6	25.5	8	300	19
SqueezeSAM (int8)	77.5	40.8	56.7	45.0	24.6	43.4	77.8	36.9	57.6	49.2	24.6	-	300	19

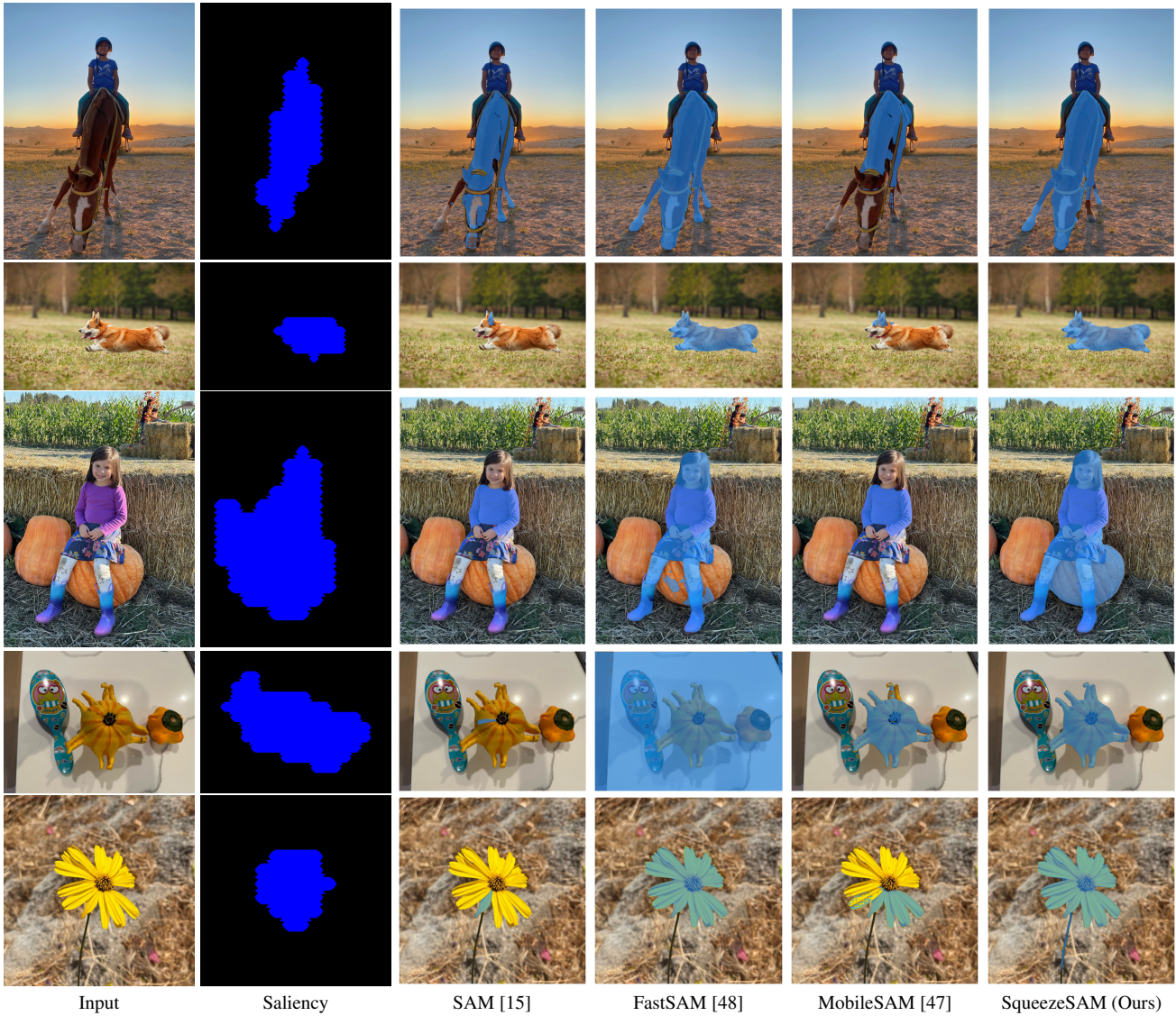


Figure 7. Qualitative comparison with SOTA methods. From left to right: (1) Input image (2) Salient blob (3-5) Other model outputs (6) Our model. Note that, while all models missed cutting out salient objects simultaneously in row 3 (pumpkin and the kid), and missed the stem and the parts of the flower in row 5, SqueezeSAM successfully cut out related parts together.

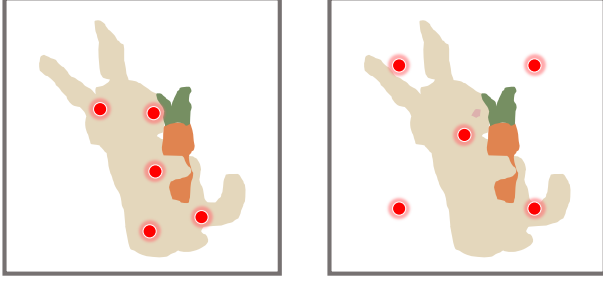


Figure 8. Left: Auto created clicks with respect to the center of mass of a blob; Right: Grid Sampling. Our proposed sampling method can provide better prompts to the interactive segmentation model than uniform sampling.

Table 2. Comparison of mIOU on COCO using 3 randomly sampled points from gt mask

	COCO			
	overall	large	medium	small
Original SAM	68.79%	76.12%	74.00%	60.52%
MobileSAM	59.69%	73.86%	66.55%	45.92%
SqueezeSAM	62.62%	67.06%	63.65%	59.30%

on person’s body. Thus, the training mask will not contain masks for tshirt if the same image has the mask for the person wearing the tshirt. As a result, the training data for the model is less ambiguous resulting in higher quality for people, pets and whole objects.

- **Outlier injection.** We occasionally sample background points which do not correspond to any object during training. This makes the model more robust to outlier points that are occasionally sampled from the saliency mask (since there is no guarantee that the saliency mask is strictly within the ground truth).
- **Center cropping around random objects.** The SA1B dataset contains many objects per image. However our usecase requires segmenting out images where there is one or two salient objects. In order to bridge the distribution gap, we randomly sample an object in the image and crop part of the image around that chosen object. We do the center cropping with 50 percent probability.

5.2. Evaluation

Internally, we collected a dataset consisting of people images. We evaluate the quality of our model on this dataset in Table 3. We find that salient SAM significantly outperforms the standard SAM. This shows that tuning for saliency is helpful for improving quality of people.

6. Saliency Evaluation

Each of our earlier evals focus on the nominal quality of the segmentation models. However, we would like to assess the

Table 3. We collected an internal dataset of images containing person masks. These images mostly contain a single person as the central entity. We find that the salient SAM variants perform significantly better than the original SAM.

Model	mIOU
Original SAM	80%
Salient SqueezeSAM	84%
Salient SqueezeSAM (ft on LVIS)	88%

quality of the segmentation models on salient objects. We use the following approach to determine whether an image has a salient object in each for each of the COCO images:

- **Saliency detection:** Run saliency detection on the image, Candidate masks for a given image: For evaluation, we use the 5k validation partition of COCO. For each image, we use the masks present in the COCO instance segmentation. Furthermore, we augment the LVIS masks and replace the corresponding COCO mask if the new LVIS mask strongly overlaps with the COCO mask ($> 80\%$). Since the LVIS masks are more fine-grained and accurate around the edges, mIOU computed over the LVIS masks gives a better indication of quality.
- **Mask selection:** Pick the ground truth mask (among the various COCO/LVIS masks available for the image) that has max IOU with the saliency mask.
- **Addressing ambiguity in the saliency model:** Sometimes the saliency mask may be multimodal and could capture multiple objects. This introduces some ambiguity in the eval since our models are learned to predict single objects only. For fair comparisons, we need to ensure that the saliency mask is attending to the specific object (chosen from step 3 above). In order to address this, we consider the chosen ground truth mask as valid only if there is sufficient intersection between the ground truth mask and the saliency mask. Our criteria for sufficient intersection is if at least 4 of the 5 gravity points chosen from the saliency mask lies within the ground truth mask. Otherwise, we consider the chosen mask to be ambiguous and all examples where there is ambiguity between the chosen ground truth mask and the saliency mask are ignored in the mIOU computation.
- Compute the mIOU over all the examples chosen from step 4 of the 5k examples

Table 4 compares various SAM models when queried using points sampled from the saliency mask. Salient SqueezeSAM dramatically outperforms the prior literature.

Higher mIOU numbers with 1 click implies that we get the right object with a single click (for example person). The salient versions can get much higher quality on salient objects with a single click (ie they are able to identify the salient object with a single click rather than requiring more clicks). As expected fine-tuning on COCO and LVIS yields

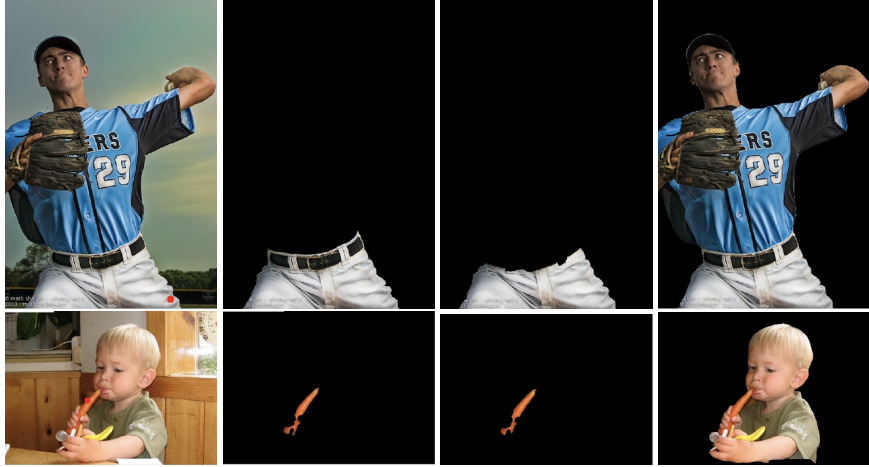


Figure 9. From left to right: (1) User-click on original image (red-dot), (2) ground-truth mask from LVIS, (3) original SAM output, (4) Salient-SqueezeSAM output. Notice that Salient-SqueezeSAM segments the all correlated objects, while other models only segment single object instances.

Table 4. Comparison of various SAM models when queried using points from the saliency mask. The test set is the large masks from COCO and LVIS validation set.

Model	1 point	3 points
Original SAM	56%	75%
Mobile SAM	58%	76%
Salient SqueezeSAM	74%	74%

the best quality due to cleaner labels and adapting to the right distribution.

7. Conclusions

In this paper, our aim is to address the problem of segmentation in resource constrained environments, such as mobile devices, especially in the context of photo editing, where users want to cutout all the interesting parts of the image simultaneously, and it is non-intuitive to select each piece separately. For example, the expected cutout from an image of depicting a person riding a bike is usually the person together with the bike, or one may want to cutout a portrait image together with the hat on their head. Unfortunately, such an output cannot be obtained from neither semantic segmentation nor instance segmentation models. Segment Anything Model is designed to be category agnostic to segment any type of object, however it focuses on individual instances, rather than the semantic saliency. Our contributions can be summarized in three folds. 1) We propose the SqueezeSAM model, which performs drastically faster while being a tiny fraction of the size of the SAM. 2) We suggest to initialize the segmentation without any user input by utilizing a SOD model, whose output is processed to

simulate the expected user-input to the segmentation model. 3) Our model can cutout correlated objects together to better capture the overall context. Because of its tiny size and tremendous speed, our Squeeze SAM can be deployed to any mobile device without throttling device resources, making it suitable for the common photo editing applications, easing the editing pipeline by auto-creating initial segmentation without requiring any user input.

References

- [1] NanoSAM. <https://github.com/NVIDIA-AI-IOT/nanosam>. Accessed: 2023-11-05.
- [2] Y.Y. Boykov and M.-P. Jolly. Interactive graph cuts for optimal boundary & region segmentation of objects in n-d images. In *Proceedings Eighth IEEE International Conference on Computer Vision. ICCV 2001*, pages 105–112 vol.1, 2001.
- [3] Han Cai, Junyan Li, Muyan Hu, Chuang Gan, and Song Han. Efficientvit: Multi-scale linear attention for high-resolution dense prediction, 2023.
- [4] Xi Chen, Zhiyan Zhao, Yilei Zhang, Manni Duan, Donglian Qi, and Hengshuang Zhao. Focalclick: Towards practical interactive image segmentation, 2022.
- [5] Dongjie Cheng, Ziyuan Qin, Zekun Jiang, Shaoting Zhang, Qicheng Lao, and Kang Li. Sam on medical images: A comprehensive study on three prompt modes, 2023.
- [6] Ruikai Cui, Siyuan He, and Shi Qiu. Adaptive low rank adaptation of segment anything to salient object detection, 2023.

- [7] Zijun Deng, Xiaowei Hu, Lei Zhu, Xuemiao Xu, Jing Qin, Guoqiang Han, and Pheng-Ann Heng. R³net: Recurrent residual refinement network for saliency detection. In *Proceedings of the Twenty-Seventh International Joint Conference on Artificial Intelligence, IJCAI-18*, pages 684–690. International Joint Conferences on Artificial Intelligence Organization, 2018.
- [8] Alexey Dosovitskiy, Lucas Beyer, Alexander Kolesnikov, Dirk Weissenborn, Xiaohua Zhai, Thomas Unterthiner, Mostafa Dehghani, Matthias Minderer, Georg Heigold, Sylvain Gelly, Jakob Uszkoreit, and Neil Houlsby. An image is worth 16x16 words: Transformers for image recognition at scale, 2021.
- [9] Chengyue Gong, Dilin Wang, Meng Li, Xinlei Chen, Zhicheng Yan, Yuandong Tian, qiang liu, and Vikas Chandra. NASVit: Neural architecture search for efficient vision transformers with gradient conflict aware supernet training. In *International Conference on Learning Representations*, 2022.
- [10] Varun Gulshan, Carsten Rother, Antonio Criminisi, Andrew Blake, and Andrew Zisserman. Geodesic star convexity for interactive image segmentation. In *2010 IEEE Computer Society Conference on Computer Vision and Pattern Recognition*, pages 3129–3136, 2010.
- [11] Agrim Gupta, Piotr Dollár, and Ross Girshick. Lvis: A dataset for large vocabulary instance segmentation, 2019.
- [12] Kaiming He, Xiangyu Zhang, Shaoqing Ren, and Jian Sun. Deep residual learning for image recognition, 2015.
- [13] Glenn Jocher, Ayush Chaurasia, and Jing Qiu. YOLO v8, 2023.
- [14] Michael Kass, Andrew P. Witkin, and Demetri Terzopoulos. Snakes: Active contour models. *International Journal of Computer Vision*, 1988.
- [15] Alexander Kirillov, Eric Mintun, Nikhila Ravi, Hanzi Mao, Chloe Rolland, Laura Gustafson, Tete Xiao, Spencer Whitehead, Alexander C. Berg, Wan-Yen Lo, Piotr Dollár, and Ross Girshick. Segment anything. In *ICCV*, 2023.
- [16] Raghuraman Krishnamoorthi. Quantizing deep convolutional networks for efficient inference: A whitepaper, 2018.
- [17] Alex Krizhevsky, Ilya Sutskever, and Geoffrey E. Hinton. Imagenet classification with deep convolutional neural networks. In *Advances in Neural Information Processing Systems 25*, pages 1097–1105. 2012.
- [18] Yin Li, Xiaodi Hou, Christof Koch, James M. Rehg, and Alan L. Yuille. The secrets of salient object segmentation, 2014.
- [19] Yanghao Li, Hanzi Mao, Ross Girshick, and Kaiming He. Exploring plain vision transformer backbones for object detection. In *Computer Vision – ECCV 2022: 17th European Conference, Tel Aviv, Israel, October 23–27, 2022, Proceedings, Part IX*, page 280–296, Berlin, Heidelberg, 2022. Springer-Verlag.
- [20] Yanyu Li, Huan Wang, Qing Jin, Ju Hu, Pavlo Chemerys, Yun Fu, Yanzhi Wang, Sergey Tulyakov, and Jian Ren. Snapfusion: Text-to-image diffusion model on mobile devices within two seconds, 2023.
- [21] Tsung-Yi Lin, Michael Maire, Serge Belongie, Lubomir Bourdev, Ross Girshick, James Hays, Pietro Perona, Deva Ramanan, C. Lawrence Zitnick, and Piotr Dollár. Microsoft coco: Common objects in context, 2015.
- [22] Tsung-Yi Lin, Piotr Dollár, Ross Girshick, Kaiming He, Bharath Hariharan, and Serge Belongie. Feature pyramid networks for object detection, 2016.
- [23] Qin Liu, Zhenlin Xu, Gedas Bertasius, and Marc Niethammer. Simpleclick: Interactive image segmentation with simple vision transformers, 2023.
- [24] Songhua Liu, Jingwen Ye, and Xinchao Wang. Any-to-any style transfer: Making picasso and da vinci collaborate, 2023.
- [25] Zhuang Liu, Hanzi Mao, Chao-Yuan Wu, Christoph Feichtenhofer, Trevor Darrell, and Saining Xie. A convnet for the 2020s, 2022.
- [26] Jonathan Long, Evan Shelhamer, and Trevor Darrell. Fully convolutional networks for semantic segmentation, 2015.
- [27] Jun Ma, Yuting He, Feifei Li, Lin Han, Chenyu You, and Bo Wang. Segment anything in medical images, 2023.
- [28] Vida Movahedi and James H. Elder. Design and perceptual validation of performance measures for salient object segmentation. *2010 IEEE Computer Society Conference on Computer Vision and Pattern Recognition - Workshops*, pages 49–56, 2010.
- [29] Konstantinos Psychogyios, Helen C. Leligou, Filisia Melissari, Stavroula Bourou, Zacharias Anastasakis, and Theodore Zahariadis. Samstyler: Enhancing visual creativity with neural style transfer and segment anything model (sam). *IEEE Access*, 11:100256–100267, 2023.
- [30] Xuebin Qin, Zichen Zhang, Chenyang Huang, Masood Dehghan, Osmar R. Zaiane, and Martin Jagersand. U²-net: Going deeper with nested u-structure for salient object detection. *Pattern Recognition*, 106: 107404, 2020.
- [31] Olaf Ronneberger, Philipp Fischer, and Thomas Brox. U-net: Convolutional networks for biomedical image segmentation, 2015.

- [32] Mehmet Sezgin and Bülent Sankur. Survey over image thresholding techniques and quantitative performance evaluation. *Journal of Electronic Imaging*, 13: 146–165, 2004.
- [33] Qihong Shen, Xingyi Yang, and Xinchao Wang. Anything-3d: Towards single-view anything reconstruction in the wild, 2023.
- [34] Ruoxi Shi, Hansheng Chen, Zhuoyang Zhang, Minghua Liu, Chao Xu, Xinyue Wei, Linghao Chen, Chong Zeng, and Hao Su. Zero123++: a single image to consistent multi-view diffusion base model, 2023.
- [35] Konstantin Sofiiuk, Ilia A. Petrov, and Anton Konushin. Reviving iterative training with mask guidance for interactive segmentation, 2021.
- [36] Ashish Vaswani, Noam Shazeer, Niki Parmar, Jakob Uszkoreit, Llion Jones, Aidan N. Gomez, Lukasz Kaiser, and Illia Polosukhin. Attention is all you need, 2017.
- [37] Lijun Wang, Huchuan Lu, Yifan Wang, Mengyang Feng, Dong Wang, Baocai Yin, and Xiang Ruan. Learning to detect salient objects with image-level supervision. In *CVPR*, 2017.
- [38] Carole-Jean Wu, David Brooks, Kevin Chen, Douglas Chen, Sy Choudhury, Marat Dukhan, Kim Hazelwood, Eldad Isaac, Yangqing Jia, Bill Jia, Tommer Leyvand, Hao Lu, Yang Lu, Lin Qiao, Brandon Reagen, Joe Spisak, Fei Sun, Andrew Tulloch, Peter Vajda, Xiaodong Wang, Yanghan Wang, Bram Wasti, Yiming Wu, Ran Xian, Sungjoo Yoo, and Peizhao Zhang. Machine learning at facebook: Understanding inference at the edge. In *2019 IEEE International Symposium on High Performance Computer Architecture (HPCA)*, pages 331–344, 2019.
- [39] Jay Zhangjie Wu, Xiuyu Li, Difei Gao, Zhen Dong, Jinbin Bai, Aishani Singh, Xiaoyu Xiang, Youzeng Li, Zuwei Huang, Yuanxi Sun, Rui He, Feng Hu, Junhua Hu, Hai Huang, Hanyu Zhu, Xu Cheng, Jie Tang, Mike Zheng Shou, Kurt Keutzer, and Forrest Iandola. Cvpr 2023 text guided video editing competition, 2023.
- [40] Qi Wu, Yuyao Zhang, and Marawan Elbatel. Self-prompting large vision models for few-shot medical image segmentation, 2023.
- [41] Defeng Xie, Ruichen Wang, Jian Ma, Chen Chen, Haonan Lu, Dong Yang, Fobo Shi, and Xiaodong Lin. Edit everything: A text-guided generative system for images editing, 2023.
- [42] Ning Xu, Brian Price, Scott Cohen, Jimei Yang, and Thomas Huang. Deep interactive object selection, 2016.
- [43] Qiong Yan, Li Xu, Jianping Shi, and Jiaya Jia. Hierarchical saliency detection. In *2013 IEEE Conference on Computer Vision and Pattern Recognition*, pages 1155–1162, 2013.
- [44] Chuan Yang, Lihe Zhang, Huchuan Lu, Xiang Ruan, and Ming-Hsuan Yang. Saliency detection via graph-based manifold ranking. In *Computer Vision and Pattern Recognition (CVPR), 2013 IEEE Conference on*, pages 3166–3173. IEEE, 2013.
- [45] Tao Yu, Runseng Feng, Ruoyu Feng, Jinming Liu, Xin Jin, Wenjun Zeng, and Zhibo Chen. Inpaint anything: Segment anything meets image inpainting, 2023.
- [46] Yi Zeng, Pingping Zhang, Jianming Zhang, Zhe Lin, and Huchuan Lu. Towards high-resolution salient object detection. In *The IEEE International Conference on Computer Vision (ICCV)*, 2019.
- [47] Chaoning Zhang, Dongshen Han, Yu Qiao, Jung Uk Kim, Sung-Ho Bae, Seungkyu Lee, and Choong Seon Hong. Faster segment anything: Towards lightweight sam for mobile applications, 2023.
- [48] Xu Zhao, Wenchao Ding, Yongqi An, Yinglong Du, Tao Yu, Min Li, Ming Tang, and Jinqiao Wang. Fast segment anything, 2023.
- [49] Tao Zhou, Yizhe Zhang, Yi Zhou, Ye Wu, and Chen Gong. Can sam segment polyps?, 2023.
- [50] Zhou, Chong and Li, Xiangtai and Loy, Chen Change and Dai, Bo EdgeSAM: Prompt-In-the-Loop Distillation for On-Device Deployment of SAM
- [51] Yunyang Xiong and Bala Varadarajan and Lemeng Wu and Xiaoyu Xiang and Fanyi Xiao and Chenchen Zhu and Xiaoliang Dai and Dilin Wang and Fei Sun and Forrest Iandola and Raghuraman Krishnamoorthi and Vikas Chandra EfficientSAM: Leveraged Masked Image Pretraining for Efficient Segment Anything